Quantum Interference Paves the Way for Long-Lived Electronic Coherences

Diptesh Dey,[1] Alexander I. Kuleff,[2] and Graham A. Worth[1,*]
[1]Department of Chemistry, University College London, 20 Gordon Street, London WC1H 0AJ, United Kingdom
[2]Theoretische Chemie, PCI, Universität Heidelberg, Im Neuenheimer Feld 229, D-69120 Heidelberg, Germany

(Received 30 March 2022; revised 2 June 2022; accepted 12 September 2022; published 18 October 2022)

The creation and dynamical fate of a coherent superposition of electronic states generated in a polyatomic molecule by broadband ionization with extreme ultraviolet pulses is studied using the multiconfiguration time-dependent Hartree method together with an ionization continuum model Hamiltonian. The electronic coherence between the hole states usually lasts until the nuclear dynamics leads to decoherence. A key goal of attosecond science is to control the electronic motion and design laser control schemes to retain this coherence for longer timescales. Here, we investigate this possibility using time-delayed pulses and show how this opens up the prospect of coherent control of charge migration phenomenon.

DOI: 10.1103/PhysRevLett.129.173203

In the past two decades, the remarkable advance in laser technology has opened the door for studying ultrafast molecular dynamics with unprecedented time resolution [1–3]. With the possibility to generate ultrashort laser pulses in the extreme ultraviolet (XUV) to soft-x-ray regime, it has become feasible to initiate, monitor, and control electronic motion on the attosecond (1 as $= 10^{-18}$ s) timescale [4–8]. Depending on the bandwidth and carrier frequency of the light source, the molecule may get ionized with the ejection of an electron from one of its molecular orbitals, creating a hole, which due to electron correlation must be represented by an electronic wave packet [9]. The hole will subsequently migrate across the molecular backbone, giving rise to the phenomenon of charge migration [9,10]. The light-induced ultrafast motion of charge and the resulting energy redistribution lies at the heart of many chemical and biochemical reactions [11,12]—leading to the concept of charge-directed reactivity [13]—with the hole migration process being identified as a promising tool to control reactivity [14].

Research in this direction began with the experimental observation of positive-charge migration in isolated peptide radical cations generated through ionization [15]. The underlying mechanism for the unexpected selectivity in photofragmentation of ionized peptides was not clear at that time. This curiosity led to several experimental [11,14,16] and theoretical [17–20] investigations suggesting that an ultrafast charge migration is the initial step in the observed charge-directed reactivity. Since the electronic motion occurs on a faster timescale than the nuclear motion, early theoretical descriptions focused on pure electron dynamics over a static nuclear framework [21–23]. They predicted that before the nuclear motion destroys the electronic coherence, oscillatory motion of the electronic density takes place, with the frequency given by the energy gap of the participating electronic states. However, the idea of separability of electron and nuclear motions was questioned [3] and the decisive role of the nuclei in the decoherence and recoherence of charge migration has been pointed out [24–26]. Based on the molecular system, the fast electronic decoherence is caused by a complex interplay of the following mechanisms [27,28]: (i) dephasing of nuclear wave packet components, (ii) loss of overlap of nuclear wave packets on different electronic states, and (iii) time evolution of electronic state populations. The first studies showed that in certain molecules and electronic states these effects can lead to decoherence times of less than 3 fs [25,27]. However, longer-lived electronic coherences have also been predicted for polyatomics [29]. To this end, the relative electronic phase plays a crucial role in achieving nuclear controllability, provided the *phase memory* persists at conical intersections [28]. An ultimate goal of attochemistry is to design and implement strategies that can modulate the coherent electron dynamics, which we aim to address here.

In this Letter, we present a systematic quantum dynamical study on the creation of a coherent superposition of electronic states, i.e., an electronic wave packet, via photoionization mediated by broadband XUV pulses. To this end, we choose propiolic acid (HC_2COOH)—the simplest acetylenic carboxylic acid—which has been argued to be suitable for an experimental study of charge migration phenomenon [29,30]. We analyze the electronic decoherence and recoherence resulting from the coupled electron-nuclear dynamics following the ejection of an outer-valence electron [26–28]. We design and implement a fairly simple but effective laser control scheme for extending the lifetime of coherences—a topic of current interest in quantum computing and light harvesting complexes [31–33]. In particular, we demonstrate that by taking advantage of the constructive (destructive) interferences

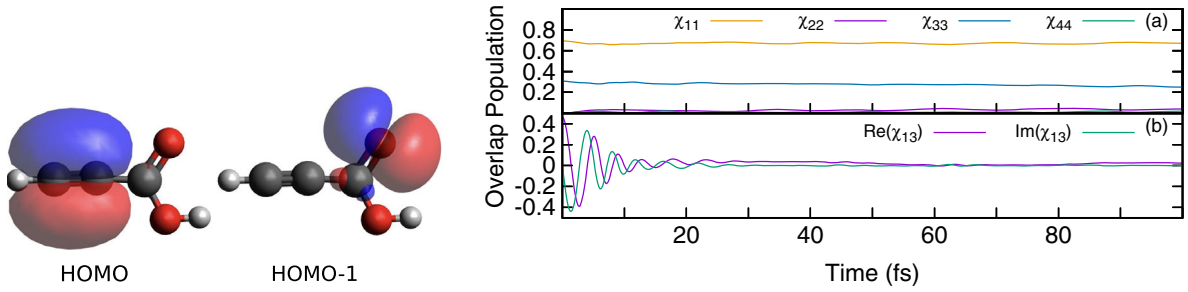

FIG. 1. The molecular orbitals of propiolic acid involved in the hole mixing are depicted on the left. Panel (a) on the right shows the evolution of state populations (χ_{ii}) of the lowest four cationic states assuming a *sudden* ionization. Panel (b) shows the nuclear overlaps (real and imaginary) between the first and third cationic states (χ_{13}) related to the electronic coherence of the system.

caused by photoexcitation with "time-delayed" pulses, longer-lived coherences can be achieved with an enhanced (reduced) degree of coherence. The simulations also demonstrate the necessity of incorporating the laser pulse explicitly in a simulation. Not only do they generate a more realistic initial state, but this offers the possibility of using different pulses to flexibly create different initial (superposition) states and thus coherences. The resulting coupled electron-nuclear dynamics can then be examined for modification of site-selective reactivity [14,34–36].

The outer-valance ionization spectrum of propiolic acid [30] consists of four close lying cationic states between 11.17 and 12.07 eV; the fifth one is located at 15.1 eV. Among these states, the first and third are a strong admixture of two one-hole ($1h$) configurations, $(15a')^{-1}$ and $(14a')^{-1}$, representing the removal of an electron from either HOMO or HOMO − 1. A spectrally broad coherent ionizing pulse of bandwidth that spans the entire range can create a coherent superposition of these two states, initiating a coherent hole dynamics which will oscillate between the carbon triple bond and carbonyl oxygen (molecular orbitals are shown in Fig. 1). Our primary interest is to investigate and probe this charge migration to achieve long-lived oscillatory motion.

The wave packet propagation is performed by numerically solving the time-dependent Schrödinger equation using the multiset, multimode formalism of the multiconfiguration time-dependent Hartree (MCTDH) algorithm [37], as implemented in the QUANTICS package [38]. The MCTDH method uses a compact expansion of the wave function in a time-dependent basis set, where both the expansion coefficients and the basis functions are propagated to optimally represent the evolving wave packet. The quadratic vibronic coupling Hamiltonian developed in Ref. [29] is employed to describe the diabatic potential energy surfaces (PESs). This assumes a Taylor expansion up to second order around the equilibrium geometry of the neutral ground state remains valid; i.e., the nuclear wave packets remain within the quadratically expanded region of the PES during the ultrafast process. It should be noted that as the potential surfaces and couplings have been calculated with the algebraic diagrammatic construction method [39], this treatment includes the full molecular electron-electron, nuclear-nuclear, as well as the nuclear-electron correlations. Further details are in the Supplemental Material [40].

A linearly polarized Gaussian pulse of peak intensity 4.8×10^{13} W/cm^2 (peak amplitude 0.037 a.u.), full width at half maximum (FWHM) of 3 fs, and a (mean) photon energy of 11.8 eV is applied. In an experiment, this intensity could lead to undesired processes such as double ionization and multiphoton excitation. In the present model, however, these channels are not present and the high field strength was chosen for numerical convenience and to clearly show the longtime coherences which are small and can be lost in the numerical noise. Within the diabatic electronic basis, the transition dipole will be a slowly varying function of the nuclear geometry and thus can be well approximated by a constant (unity). The simulation details are provided in the Supplemental Material [40]. The ejected photoelectron is taken into account by including the ionization continua through a discretization by a discrete-variable representation [41,42]. This balances the energy to allow the evolving nuclear wave packet to access the correct vibrational eigenstates of the ion, but does not treat the electron explicitly and therefore ignores any entanglement between the outgoing electron and the molecular ion. Assuming the validity of the model Hamiltonian (small nuclear displacements), this missing entanglement is the only approximation being made in our calculations. This entanglement has been observed, in particular with slow photoelectrons [46,47], and can lead to recollisions which affect the system dynamics. However, quantum-classical simulations of the water cation indicate that the photoelectron-ion coupling decoheres within 50–100 as, much shorter than the timescale of our simulations [48].

The ultrafast charge dynamics in time and space can be visualized by computing the *hole density* defined as the difference between the electronic densities of the neutral and the cation [9,49]. The time-dependent overlaps between the nuclear wave packets evolving on different electronic states $[\chi_{ij}(t) = \langle \chi_i(t) | \chi_j(t) \rangle]$ provide an indication of the electronic coherence in the system [29]. The displacements of vibrational normal modes around their

equilibrium configuration result in damping of the electron density oscillations indicating the loss of coherence to be a multimodal effect. The Supplemental Material [40] sheds light on this through incorporation of "only 5 modes" versus "all 15 modes" of HC_2COOH.

The onset of charge migration is often modeled by assuming a "sudden" ionization, with the vertical excitation of the nuclear wave packet from the neutral ground state to the manifold of cationic states [29,35]. Since the first and third cationic states are linear combinations of two $1h$ configurations [30], a short-time impulsive excitation will simultaneously populate both states, creating the initial superposition state. Figure 1 depicts such a situation by considering a 66.7% and 33.3% superposition of the two states. Figure 1(a) shows the temporal evolution of the state populations χ_{ii} of the lowest four cationic states. The nuclear overlap between the first and third cationic states (i.e., the off-diagonal element of the electronic density matrix) χ_{13} is shown in Fig. 1(b). The oscillation period of ~6.2 fs corresponds to the energy gap between the first and third ionic states, which is 0.67 eV. The coherent oscillations are found to decrease with time as they depend on the nuclear geometry (see also Ref. [29]).

Let us now examine the charge dynamics by explicitly including the ionization step with a laser field exciting the neutral molecule to the ion states with our simple discretized continua model of the outgoing electron kinetic energy to correctly describe the energetics. Figure 2 shows the influence of an ionizing XUV pulse on the creation of a superposition state and the charge migration initiated by it. The population of the neutral ground state (χ_{00}) decays and the first (χ_{11}) and third (χ_{33}) cationic state populations rise gradually and then stay more or less constant. The nuclear overlap between the first and third cationic states χ_{13} indicates the electronic coherence of the system—rise, decay, and revivals. The coherence is maintained up to 35 fs, then recurrences are observed at around 50 and 70 fs. The revivals indicate the role of the nuclei in conserving the "phase memory" after the initial decoherence sets in. Comparison with Fig. 1 portrays the differences that result from the theoretical models: "sudden" versus "laser induced." In contrast to quasi-field-free sudden ionization, in the laser-driven ionization the phase associated with the electronic wave packet is composed of the phases of the neutral ground state wave packet and the optical field. This results in the variation in the magnitude of the nuclear overlaps in the two cases. To this end, the initial phase of the hole wave packet will depend strongly on the orientation of the molecule with respect to the laser polarization [50].

Having established the laser-induced coherent superposition states and monitored their evolution or overlaps, the next question is as to whether it is possible to manipulate the coherent signal to extend its lifetime. To do this, a series of calculations was performed with a train of twin (two identical) pulses, phase locked with varying time delays (τ). Figure 3 shows the creation, evolution of

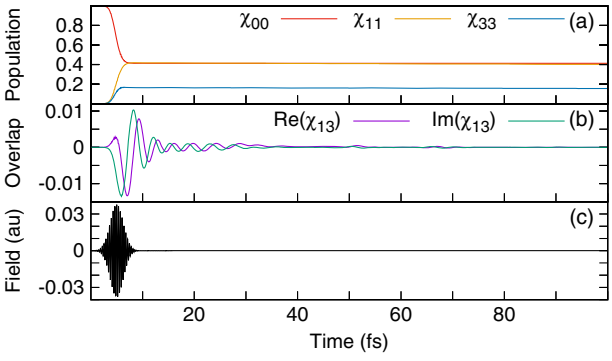

FIG. 2. Upper panel: evolution of state populations of the neutral ground state (χ_{00}) and the first (χ_{11}) and third (χ_{33}) cationic states of propiolic acid in the presence of an XUV pulse. Middle panel: nuclear overlaps (real and imaginary) between the first and third cationic states (χ_{13}) related to the electronic coherence of the system. Lower panel: XUV pulse of center frequency ~105 nm, width (FWHM) of 3 fs and peaked at 5 fs.

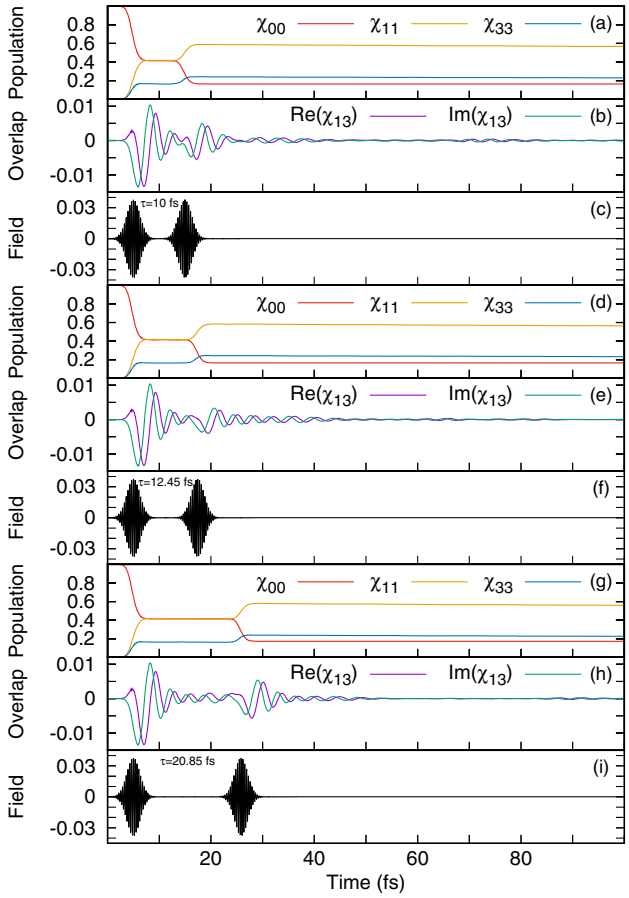

FIG. 3. State populations, nuclear overlaps (coherence), and electric field as in Fig. 2, except that the laser pulse now consists of two identical pulses with a separation of 10 fs (a)–(c), 12.45 fs (d)–(f), and 20.85 fs (g)–(i).

the state populations, and the associated nuclear overlaps in the presence of a train of pulses with three different time delays between the pulse centers. Figures 3(a)–3(c) correspond to $\tau = 10$ fs, chosen to avoid significant pulse overlap. The population transfer occurs in a stepwise fashion with the first pulse playing the major role. Although the pulse sequence is over at 20 fs, the coherence remains until 45 fs. Interestingly, also a stronger revival is seen which lasts for a prolonged time (from 70 to 80 fs). Figure S2 of the Supplemental Material [40] provides a detailed comparison of the revivals. The time-delayed pulse therefore leads to an enhanced control over the charge migration process.

The mechanism behind this enhancement is quantum (amplitude) interference [51–53]. The first pulse generates an electronic wave packet on the cationic states whose internal phase evolves with certain phase velocities. This wave packet then interferes (either constructively or destructively) with another wave packet launched by the delayed pulse to result in an enhancement or suppression of the coherence. The shift or delay in time thereby introduces a certain phase shift which corresponds to a linear phase modulation, i.e., a linear spectral chirp in the spectral regime, opening avenues for coherent control [54,55]. Thus, a simple modulation of the time delay between the pulses imprints a relative phase between the electronic states which results in an alteration of the coherence and thereby potentially steering the nuclear wave packet toward a desired rearrangement.

Figures 3(d)–3(i) elaborate on this where for time delays of 12.45 and 20.85 fs a suppression and enhancement (respectively) of the initial coherent signal is noted, but with weaker recurrences. Interestingly, a time delay of 20.85 fs does not extend the initial coherence much past 50 fs, but the recurrence is now seen at much longer times, around 90 fs. The complete sequence of time-delayed snapshots starting from $\tau = 10$ fs with gradual increments of 350 as provides a detailed insight (see movie in the Supplemental Material [40]). It should be noted that the second pulse in the train can in principle also induce a population transfer from the cationic states populated by the first pulse to higher lying cationic states. These processes are likely to be weak and are not expected to influence the degree of coherence between the first and the third states. That is why they are excluded in the present model. The potential importance of this effect should be, however, further investigated.

Figure 4 illustrates the electron-hole density of HC_2COOH upon photoionization with [Fig. 4(a)] a single XUV pulse and [Fig. 4(b)] a sequence of two XUV pulses ($\tau = 10$ fs). The electronic wave packet formed by the superposition starts on the carbon triple bond, but migrates during the formation to place the hole with a strong signal on the carboxyl end of the molecule. The hole is then seen to oscillate between the two ends of the molecule until, with

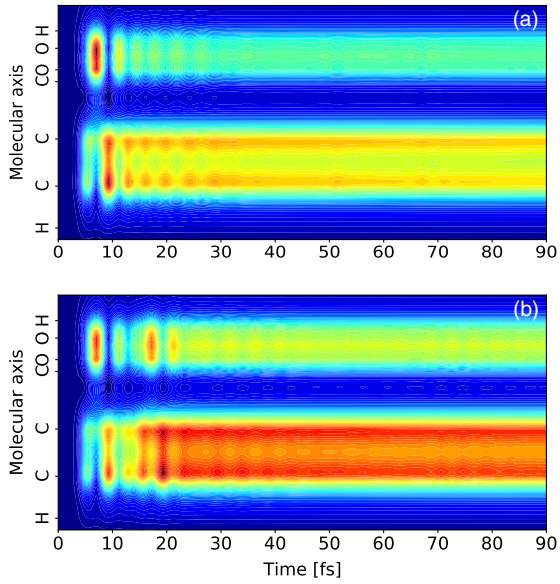

FIG. 4. Evolution of the hole density upon photoionization with a single XUV pulse centered at 5 fs (upper panel) and a sequence of two XUV pulses centered at 5 and 15 fs, respectively (lower panel).

the onset of the electronic decoherence, the hole gradually settles down and gets delocalized over the molecule with its largest fraction localized on the carbon triple bond. The longer coherence time of the twin pulse excitation is also seen in the longer time of the hole oscillations.

Our results complement previous studies. For example, it has been shown previously that the initial degree of coherence depends on the choice of laser parameters [46]: it rises with either decreasing pulse duration (for a fixed photon energy) or increasing mean photon energy (for a fixed pulse duration) of the ionizing pulse. A short pulse in the time domain is composed of a wide frequency distribution in the spectral domain. Upon excitation it creates a broad (narrow) wave packet in energy (time) domain and this will stay relatively narrow during the subsequent evolution in time, thereby accounting for a larger coherence.

To conclude, this Letter reports the first quantum-dynamical study with the explicit inclusion of a laser field to create a coherent superposition of cationic states in a polyatomic molecule. A comparison with the widely used quasi-field-free sudden ionization approach indicates a significant variation in the degree of coherence. The electronic wave packet obtained via sudden ionization carries only the amplitude and phase information of the neutral ground state, whereas with laser-driven ionization an additional amplitude and phase information of the applied electric field gets imprinted in the superposition state. Since the laser-induced state couplings dictate the formation of the initial superposition of states and their mixing ratio, the resulting dynamics gets further enriched.

The initial electronic wave packet can thus be generated in a controlled fashion which will induce electron dynamics that can steer a desired nuclear rearrangement (provided the electronic coherence survives till the onset of nuclear motion [56]).

To address the possibility of retaining electronic coherences for longer time periods, we invoked a simple two-pulse laser excitation scheme. We demonstrated that the optical and wave packet phases play a vital role in achieving this goal and the degree of coherence can be enhanced or suppressed based on quantum (amplitude) interferences. With a pulse shaper capable of amplitude and phase shaping even better control must potentially be achievable. Thereby a longer-lived coherence can be induced following this excitation scheme. These results have far-reaching consequences beyond a particular molecular system and on top of the natural dynamics of the system. Previous analysis has shown that the (de) coherence and revivals indicate the role of nuclei in charge migration dynamics [26,27]. For example, in electronic states with similar character, as in propiolic acid, the electronic coherence survives for a longer time than states of differing character even in the absence of a laser pulse [27]. Previous investigations have also looked into the possibility of steering the charge migration dynamics in a traditional photochemistry sense by applying a "control" pulse close to a conical intersection [57,58]. Few-cycle pulses also offer the possibility of achieving quantum-interference control by varying the carrier-envelope phase —the temporal offset between the maxima of the pulse envelope and the optical cycle [59]. With XUV pulses composed of a large number of optical cycles within the pulse envelope, almost no alteration in the state populations is noted.

Our ability to control quantum coherence opens new avenues and we believe that it will stimulate researchers to conduct further studies on ultrafast charge migration. These exact quantum-mechanical calculations will also serve as benchmark for future development in this area.

D. D. is grateful to Professor Jon Marangos for illuminating discussions and to Dr. Nikolay Golubev for providing the code to calculate the hole density. The research leading to these results has received funding from the European Union's Horizon 2020 research and innovation programme under the Marie Sklodowska-Curie Grant Agreement No. 892554. A. I. K. thanks the DFG for the financial support provided through the QUTIF Priority Programme. G. A. W. thanks the EPSRC for funding under Grant No. EP/T006560/1.

*g.a.worth@ucl.ac.uk

[1] M. Hentschel, R. Kienberger, Ch. Spielmann, G. A. Reider, N. Milosevic, T. Brabec, P. Corkum, U. Heinzmann, M. Drescher, and F. Krausz, Nature (London) **414**, 509 (2001).
[2] F. Calegari, D. Ayuso, A. Trabattoni, L. Belshaw, S. De Camillis, S. Anumula, F. Frassetto, L. Poletto, A. Palacios, P. Decleva, J. B. Greenwood, F. Martín, and M. Nisoli, Science **346**, 336 (2014).
[3] S. R. Leone *et al.*, Nat. Photonics **8**, 162 (2014).
[4] F. Krausz and M. Ivanov, Rev. Mod. Phys. **81**, 163 (2009).
[5] E. Goulielmakis, Z.-H. Loh, A. Wirth, R. Santra, N. Rohringer, V. S. Yakovlev, S. Zherebtsov, T. Pfeifer, A. M. Azzeer, M. F. Kling, S. R. Leone, and F. Krausz, Nature (London) **466**, 739 (2010).
[6] K. P. Singh, F. He, P. Ranitovic, W. Cao, S. De, D. Ray, S. Chen, U. Thumm, A. Becker, M. M. Murnane, H. C. Kapteyn, I. V. Litvinyuk, and C. L. Cocke, Phys. Rev. Lett. **104**, 023001 (2010).
[7] H. Timmers, N. Shivaram, and A. Sandhu, Phys. Rev. Lett. **109**, 173001 (2012).
[8] D. Dey, D. Ray, and A. K. Tiwari, J. Phys. Chem. A **123**, 4702 (2019).
[9] L. S. Cederbaum and J. Zobeley, Chem. Phys. Lett. **307**, 205 (1999).
[10] A. I. Kuleff and L. S. Cederbaum, J. Phys. B **47**, 124002 (2014).
[11] H. J. Wörner *et al.*, Struct. Dyn. **4**, 061508 (2017).
[12] V. May and O. Kühn, *Charge and Energy Transfer Dynamics in Molecular Systems*, 3rd ed. (Wiley-VCH, Weinheim, 2011).
[13] F. Remacle, R. D. Levine, and M. A. Ratner, Chem. Phys. Lett. **285**, 25 (1998).
[14] R. Weinkauf, E. W. Schlag, T. J. Martinez, and R. D. Levine, J. Phys. Chem. A **101**, 7702 (1997).
[15] R. Weinkauf, P. Schanen, A. Metsala, E. W. Schlag, M. Bürgle, and H. Kessler, J. Phys. Chem. **100**, 18567 (1996).
[16] L. Lehr, T. Horneff, R. Weinkauf, and E. W. Schlag, J. Phys. Chem. A **109**, 8074 (2005).
[17] J. Breidbach and L. S. Cederbaum, J. Chem. Phys. **118**, 3983 (2003).
[18] F. Remacle and R. D. Levine, Z. Phys. Chem. **221**, 647 (2007).
[19] S. Lünnemann, A. I. Kuleff, and L. S. Cederbaum, Chem. Phys. Lett. **450**, 232 (2008).
[20] S. Sun, B. Mignolet, L. Fan, W. Li, R. D. Levine, and F. Remacle, J. Phys. Chem. A **121**, 1442 (2017).
[21] A. I. Kuleff and L. S. Cederbaum, Chem. Phys. **338**, 320 (2007).
[22] V. Despré, A. Marciniak, V. Loriot, M. C. E. Galbraith, A. Rouzée, M. J. J. Vrakking, F. Lépine, and A. I. Kuleff, J. Phys. Chem. Lett. **6**, 426 (2015).
[23] M. Lara-Astiaso *et al.*, J. Phys. Chem. Lett. **9**, 4570 (2018).
[24] M. Vacher, L. Steinberg, A. J. Jenkins, M. J. Bearpark, and M. A. Robb, Phys. Rev. A **92**, 040502(R) (2015).
[25] C. Arnold, O. Vendrell, and R. Santra, Phys. Rev. A **95**, 033425 (2017).
[26] D. Jia, J. Manz, and Y. Yang, J. Phys. Chem. Lett. **10**, 4273 (2019).
[27] M. Vacher, M. J. Bearpark, M. A. Robb, and J. P. Malhado, Phys. Rev. Lett. **118**, 083001 (2017).
[28] C. Arnold, O. Vendrell, R. Welsch, and R. Santra, Phys. Rev. Lett. **120**, 123001 (2018).
[29] V. Despré, N. V. Golubev, and A. I. Kuleff, Phys. Rev. Lett. **121**, 203002 (2018).

[30] N. V. Golubev, V. Despré, and A. I. Kuleff, J. Mod. Opt. **64**, 1031 (2017).
[31] G. S. Engel, T. R. Calhoun, E. L. Read, T.-K. Ahn, T. Mančal, Y.-C. Cheng, R. E. Blankenship, and G. R. Fleming, Nature (London) **446**, 782 (2007).
[32] N. Lambert, Y.-N. Chen, Y.-C. Cheng, C.-M. Li, G.-Y. Chen, and F. Nori, Nat. Phys. **9**, 10 (2013).
[33] P. Wang, C.-Y. Luan, M. Qiao, M. Um, J. Zhang, Y. Wang, X. Yuan, M. Gu, J. Zhang, and K. Kim, Nat. Commun. **12**, 233 (2021).
[34] M. Olivucci, T. Tran, G. A. Worth, and M. A. Robb, J. Phys. Chem. Lett. **12**, 5639 (2021).
[35] T. Tran, G. A. Worth, and M. A. Robb, Commun. Chem. **4**, 48 (2021).
[36] G. K. Paramonov, T. Klamroth, H. Z. Lu, and A. D. Bandrauk, Phys. Rev. A **98**, 063431 (2018).
[37] M. H. Beck, A. Jäckle, G. A. Worth, and H. D. Meyer, Phys. Rep. **324**, 1 (2000).
[38] G. A. Worth, K. Giri, G. W. Richings, I. Burghardt, M. H. Beck, A. Jäckle, and H.-D. Meyer, *The Quantics Package*, Version 1.2 (University of Birmingham, Birmingham, UK, 2016).
[39] J. Schirmer, A. B. Trofimov, and G. Stelter, J. Chem. Phys. **109**, 4734 (1998).
[40] See Supplemental Material at http://link.aps.org/supplemental/10.1103/PhysRevLett.129.173203 for more details on the model, methods used, and further analysis and results, which includes Refs. [9,29,37,41–45].
[41] M. Seel and W. Domcke, J. Chem. Phys. **95**, 7806 (1991).
[42] G. A. Worth, R. E. Carley, and H. H. Fielding, Chem. Phys. **338**, 220 (2007).
[43] H.-D. Meyer, U. Manthe, and L. S. Cederbaum, Chem. Phys. Lett. **165**, 73 (1990).
[44] G. A. Worth, H.-D. Meyer, and L. S. Cederbaum, J. Chem. Phys. **109**, 3518 (1998).
[45] H. Köppel, W. Domcke, and L. S. Cederbaum, Adv. Chem. Phys. **57**, 59 (1984).
[46] S. Pabst, L. Greenman, P. J. Ho, D. A. Mazziotti, and R. Santra, Phys. Rev. Lett. **106**, 053003 (2011).
[47] M. Nisoli, P. Decleva, F. Calegari, A. Palacios, and F. Martín, Chem. Rev. **117**, 10760 (2017).
[48] C. Arnold, C. Larivière-Loiselle, K. Khalili, L. Inhester, R. Welsch, and R. Santra, J. Phys. B **53**, 164006 (2020).
[49] J. Breidbach and L. S. Cederbaum, J. Chem. Phys. **118**, 3983 (2003).
[50] P. M. Kraus *et al.*, Science **350**, 790 (2015).
[51] N. F. Scherer, R. J. Carlson, A. Matro, M. Du, A. J. Ruggiero, V. Romero-Rochin, J. A. Cina, G. R. Fleming, and S. A. Rice, J. Chem. Phys. **95**, 1487 (1991).
[52] H. Goto, H. Katsuki, H. Ibrahim, H. Chiba, and K. Ohmori, Nat. Phys. **7**, 383 (2011).
[53] R. Hildner, D. Brinks, J. B. Nieder, R. J. Cogdell, and N. F. van Hulst, Science **340**, 1448 (2013).
[54] M. Shapiro and P. Brumer, *Principles of the Quantum Control of Molecular Processes* (Wiley, New York, 2012).
[55] D. Dey, A. K. Tiwari, and N. E. Henriksen, Chem. Phys. Lett. **716**, 131 (2019).
[56] I. C. D. Merritt, D. Jacquemin, and M. Vacher, J. Phys. Chem. Lett. **12**, 8404 (2021).
[57] N. V. Golubev and A. I. Kuleff, Phys. Rev. A **91**, 051401(R) (2015).
[58] T. Tran, A. J. Jenkins, G. A. Worth, and M. A. Robb, J. Chem. Phys. **153**, 031102 (2020).
[59] F. Schüppel, T. Schnappinger, L. Bäuml, and R. de Vivie-Riedle, J. Chem. Phys. **153**, 224307 (2020).